Sains Malaysiana 52(5)(2023): 1557-1565
http://doi.org/10.17576/jsm-2023-5205-17

Powder Injection Moulded Ti6Al4V-HA Composite for Implants

(Pengacuan Suntikan Serbuk Komposit Ti6Al4V-HA untuk Implan)

NURUL NADIAH MAHMUD[1,4,*], ABU BAKAR SULONG[2] & KEI AMEYAMA[3]

[1]Research Organization of Science and Technology, Ritsumeikan University, 1-1-1 Noji Higashi, Kusatsu City, Shiga, 525-8577, Japan
[2]Department of Mechanical and Manufacturing Engineering, Faculty of Engineering and Built Environment, Universiti Kebangsaan Malaysia, 43600 UKM Bangi, Selangor Darul Ehsan, Malaysia
[3]Department of Mechanical Engineering, Ritsumeikan University, 1-1-1 Noji Higashi, Kusatsu City, Shiga, 525-8577, Japan
[4]Universiti Kuala Lumpur Malaysia France Institute, 43650 Bandar Baru Bangi, Selangor Darul Ehsan, Malaysia

Received: 4 November 2022/Accepted: 11 April 2023

ABSTRACT

Powder injection moulding (PIM) is widely used to produce complex shapes of Titanium and its alloys. Ti6Al4V-HA feedstocks at 63, 64 and 66 vol.% were produced by combining a Ti6Al4V-HA powder mixture (90:10 wt.%) with a binder system containing palm stearin (PS) and low-density polyethylene (LDPE). Binder system consisted with 60 wt.% of PS and 40 wt.% of LDPE. All powder loading materials were successfully injection moulded into the shape of a tension bar. Following that, all powder loadings were successfully debound in solvent and thermal methods. Based on SEM observation that 66 vol.% powder loading demonstrated homogenized distribution of powder and binder. Hence, 66 vol.% powder loading was selected for further process sintering at 1300 ºC, and its bending strength was evaluated. Sintered Ti6Al4V-HA with porous structure has Young's modulus of 11 GPa, within the Young modulus of bone (10 to 30 GPa). The results of this study indicate that sintered Ti6Al4V-HA has potential as an implant material.

Keywords: Composite; hydroxyapatite; powder injection moulding; Ti6Al4V

ABSTRAK

Pengacuan suntikan serbuk (PIM) digunakan secara meluas untuk menghasilkan bentuk kompleks daripada Titanium dan aloinya. Bahan suapan Ti6Al4V-HA pada 63, 64 dan 66 vol.% dihasilkan dengan menggabungkan campuran serbuk Ti6Al4V-HA (90:10 wt.%) dengan sistem pengikat yang mengandungi stearin sawit (PS) dan polietilena berketumpatan rendah (LDPE). Sistem pengikat terdiri daripada 60 wt.% daripada PS dan 40 wt.% daripada LDPE. Semua pemuatan serbuk berjaya disuntik ke dalam bentuk bar regangan. Selepas itu, semua pemuatan serbuk berjaya dinyahikat dalam kaedah pelarut dan haba. Berdasarkan pemerhatian SEM, 66 vol.% pemuatan serbuk menunjukkan taburan serbuk dan pengikat yang homogen. Oleh itu, pemuatan serbuk 66 vol.% telah dipilih untuk proses selanjutnya pensinteran pada 1300 ºC dan kekuatan lenturnya dinilai. Jasad sinter Ti6Al4V-HA dengan struktur liang mempunyai modulus Young sebanyak 11 GPa, berada dalam modulus Young tulang (10 sehingga 30 GPa). Hasil kajian ini menunjukkan jasad sinter Ti6Al4V-HA mempunyai potensi untuk digunakan sebagai bahan implan.

Kata kunci: Hidrosiapatit; komposit; pengacuan suntikan serbuk; Ti6Al4V

INTRODUCTION

Powder injection moulding (PIM) has been introduced and widely accepted because of its ability to produce near net-shape products with complex shape made of metals and ceramics for high-performance applications. The PIM technique was introduced as an alternative processing technique in the automotive industry (Hausnerova et al. 2011). The combination of plastic injection moulding

and powder metallurgy (PM) leads to the investigation of PIM, which is capable of mass-producing geometrical components, resulting in a lower production costs. PIM's four major processes are mixing, injection moulding, debinding and sintering. PIM-produced parts or products are widely used in a variety of fields, including high-temperature applications, automotive, electronics, and medical devices.

In the beginning, 316L stainless steel and Co-Cr alloys are used in biomedical applications. However, elements such as Ni, Cr and Co are released due to low corrosion resistance in the body environment (Eliaz 2019; Okazaki & Gotoh 2005), which will cause skin diseases and have found to be toxicity and carcinogenic with strong evidence was found in several animal studies (McGregor et al. 2000). Furthermore, both 316L stainless steel and Co-Cr alloys exhibit a much higher Young's modulus than bone which initiate the phenomenon of stress shielding which is as much as to be avoided to prevent implants' loosening and dead of surrounding tissue. As a result, Ti and Ti-based alloys are becoming more popular for use as biomedical products in comparison to stainless steel and Co-Cr alloy (Niespodziana 2019) due to their favourable properties such as high strength, low density (high specific strength), high corrosion resistance, biological inertness and biocompatible, and low Young's modulus (Niinomi 2002). Nonetheless, metallic implants have issues with osseointegration properties and corrosion, which causes material implant disintegration and implant loosening (Crosby et al. 2014). Several improvements to osseointegration problems have been developed, such as coatings or the fabrication of composites with bioactive materials (Mohd Yusuf et al. 2021; Najlaa Nazihah et al. 2018). HA is one of the most used bioactive material (Tecu et al. 2018) due to it shows biological compatibility and exhibit good osseointegration with the bone. HA-coated implants showed uneven coating on the complex and geometrical shape, as well as coating material detachment from the implants, which will lose their function (Miranda et al. 2016). Composites fabrication of metallic materials and HA can be a solution to overcome problems raised during coating. Ti6Al4V with uniformly distributed HA was beneficial for osseointegration activities (Miranda et al. 2016). It has been reported that the bone's cell formation was observed on Ti-HAP-coated implants compared to Ti (Kohri et al. 1990), indicates that the presence of HA aids and significantly improves Ti6Al4V bioactivity (Faezeh et al. 2022; Krishna & Suresh 2022).

The current study aims to develop a Ti6Al4V-HA composite as a biomaterial alternative by combining Ti6Al4V's satisfactory mechanical properties and HA's excellent osseoconductive properties. PIM appears to be a viable alternative method for producing Ti6Al4V-HA composites for a variety of practical reasons, including the ability to mass produce highly complex shapes at a lower cost. The sintering parameters for Ti6Al4V-HA composite is challenging due to HA prone to decompose at high sintering temperature meanwhile low sintering temperature is not favourable for Ti6Al4V. The pre-sintering step helped to enhance the sintered part density at initial stage of sintering (German & Bose 1997). Despite of mechanical properties, physical properties of sintered part also important to be analysed to ensure the suitability and possibility of the products to be used as biomaterials.

Materials and Methods

Raw materials used in the present study is concluded in Table 1. The critical powder volume percentage (CPVP) was determined at 68 vol. % (Nurul Nadiah et al. 2021b). Feedstocks were develop at powder loading below the CPVP value at 63, 64 and 66 vol.%. This is because the moulding process is usually performed at powder loading with slightly higher binder composition than measured at critical level. When the powder ratio exceeds the CPVP value, there is insufficient binder to prevent voids, which causes difficulty during injection moulding. Excess binder state, on the other hand, causes flashing during injection moulding and inhomogeneity in the feedstock. Ti6Al4V-HA powder at powder ratio of 90:10 wt.% was mixed with 60 wt.% of palm stearin and 40 wt.% of polyethylene. The mixed powder of Ti6Al4V-HA and binders at each powder loading were then placed into mixer (model W50EHT, Brabender GmbH & Co, Germany) at 150 °C with speed of 25 rpm for 45 min to prepare each feedstock. The feedstock for each powder loading were injected into a tensile bar shape using horizontal injection molding machine (model Dr Boy 22A, Boy Spritzgiessautomaten, Germany) at 170 °C. The pressure was set to 15 MPa, the filling time was set to 2 s, and the mould temperature was set to 70 °C. Debinding process were carried out initially in heptane solution at 60 °C for 6 hours by using Furnace Dryer WTB Binder (model 950204). Subsequently, the solvent-debound green part was thermally debound under argon atmosphere at 500 °C for 3 h by using split furnace (model RSAT-800, RS Advanced Technology, Malaysia).

The heating rate was maintained at 3 °C/min. Debound part was then sintered by using vacuum sintering furnace Korea VAC-TEC model VTC 500HTSF at vacuum level of minus six bar. Sintering temperature was conducted at 1300 °C. The heating rate and cooling rate was maintained at 3 °C per minute and 5 °C per minute, respectively, as shown in Figure 1. The pre-sintered step could enhance the density of sintered part at initial stage of sintering at 70 % and further increased during sintering (German & Bose 1997).

TABLE 1. Raw materials

Material	Chemical formula	Density	Source
Titanium	Ti6Al4V	4.35 g/cm^3	Vistec Technology Services
Hydroxyapatite	$Ca_{10}(PO_4)_6(OH)_2$	3.13 g/cm^3	Sigma Aldrich (M) Sdn. Bhd
Palm Stearin	$CH_3(CH_2)_{14}COOH$	0.89 g/cm^3	The Polyolefin Company (Singapore) Pte.Ltd
LDPE	$(C_2H_4)n$	0.91 g/cm^3	Sime Darby Kempas Sdn. Bhd

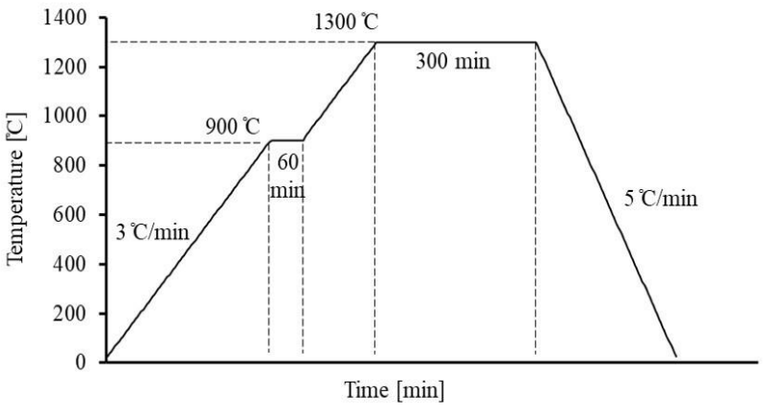

FIGURE 1. Heating profile of sintering process

Results and Discussion

Figure 2 shows the SEM images of Ti6Al4V and HA powders used in this study. Based on the SEM image of Ti6Al4V in Figure 2(a), the particles are uneven in sizes and irregular in shapes. Meanwhile, as illustrated in Figure 2(b), HA powder had agglomerated into sub-micron clusters. Based on the CPVP value of 68 vol.%, feedstock with powder loadings of 63, 64, and 66 vol.% were prepared. It is appropriate where the binder content in injection moulding is typically 30-50 vol.% (Meshalkin & Belyakov 2020). Torque versus time graph during mixing process of each Ti6Al4V-HA feedstocks are shown in Figure 2(c). The torque value initially increased due to the addition of powder and binder to produce feedstock. Subsequently, the torque decreased as the blades rotated over time, until it was nearly constant. Feedstocks with a homogenized distribution were obtained when the torque value reached a constant value (Abdoos, Khorsand & Yousefi 2014). This is due

to the fact that when the feedstock contained a uniform distribution of powder and binder, the power required for mixing remained constant. All feedstocks reached a steady state torque value in less than 10 min, which was consistent with previous work claiming that the steady state in a mixing time can be reached in less than 30 min (Thomas-Vielma et al. 2008). It has been discovered that the higher the powder loading, the greater the value of the mixing torque. Supati et al. (2000) made a similar observation about mixing behaviour at different powder loadings. As the powder loading increases, so does the mixing torque. The higher powder loading had a lower binder composition, resulting in a high powder intensity in the feedstock. As a result, increased powder loading caused more friction and resistance on the rotor blades.

Figure 3 shows green part with tensile bar shape was successfully obtained after injection moulding. According to Figure 3(a) to 3(c) of SEM images of the Ti6Al4V-HA green parts of each powder loading, it can be seen that at 63 vol.% powder loading, there was agglomeration of particles and binders. Some parts had particles-riched area of particles while some parts had binder-riched area. As the powder ratio increased to 64 vol.%, the separated area of powder and binder was less spotted. It can be seen that homogenized distribution of powder and binder was obtained at 66 vol.% of powder loading. Homogenized distribution of powder and binder is important. This is due to the fact that an inhomogeneous feedstock causes density gradients within the moulded part, which causes distortion (Supati et al. 2000). Moreover, the inhomogeneity of the feedstocks will remain until the sintering and thus sintered part will also contain an inhomogenous microstructure and binder-riched area will remain as large pores. It can be concluded that the current study demonstrated an adequate binder ratio that resulted in homogenized powder and binder distribution at 66 vol.%. Following that, the green parts were subjected into debinding process via solvent and thermal which is in consistent with other research work (Farhana et al. 2013). Lin et al. (2018) powder injection molding (PIM carried out both solvent and thermal debinding on 67 vol.% Ti6Al4V green part. Usually, debinding process are carried out sequentially for feedstocks containing multicomponents binder. This is to prevent debound parts to be collapsed during debinding and sintering. Low-melting-point polymer is usually eliminated earlier during solvent debinding or by thermal debinding at low temperature (Thavanayagam et al. 2015). Therefore, Ti6Al4V-HA green parts were subjected on solvent debinding at earlier stage for PS removal. Subsequently, for high-melting-point binder of LDPE were removed during thermal debinding to retain and maintain the shape of the moulded part.

Figure 3(d) to 3(f) shows the SEM images of solvent debound part of each powder loading. It is observed that capillaries or open pores are created after solvent debinding as mark with yellow arrows. This is attributed to first stage of debinding provides pathway for removal of backbone binder (high-melting-point binder which was LDPE as backbone binder in this current study). Based on SEM images of thermal debound parts in Figure 3(g) to 3(i), pores were also observed after removal of LDPE at 63 and 64 vol.% of powder loading. Small pores were visible as the powder loading increases. Feedstock at 66 vol.% powder loading with small pores were seen indicating that binders were homogenizedly distributed in the feedstock system. Minimal pores after thermal debound is important to help in sinterability of powder particles and high density of the final product. This is because small pores could be eliminated during sintering by the grain growth and necking of the Ti6Al4V and HA particles. The debound parts known as brown parts demonstrated fragile and brittle characteristics due to the presence of large voids as well as there was no interparticle bonding occurred during thermal debinding. As a result, no mechanical testing was performed on debound parts. It was determined that binders left in the brown parts was approximately 3.4 ± 0.66%. Farhana et al. (2013) reported that PS was removed from 83 to 92% during solvent debinding and polypropylene (PP) was removed 94 to 98% during thermal debinding. The current result showed that 96.6% of binders were removed, which is consistent with other reported works. Nevertheless, those remaining binders in the debound part function to maintain the shape until sintering process.

Powder loading at 66 vol. % was taken for further analysis of sintering due to it had highest powder loading as well as the homogenized distribution of powder and binder within the feedstock. Figure 4(a) depicts SEM images for sintered Ti6Al4V-HA at 1300 °C. It can be seen that the sintered part had pores and appeared to be interconnected. This type of interconnected porosity microstructure is critical for bone ingrowth into implants. Interconnected porosity is required for mineral and blood circulation into the bones, as well as bone ingrowth (Otsuki et al. 2006). Interconnected porosity are also beneficial to improve bonding between bone and implant which can strengthen the position of implant and

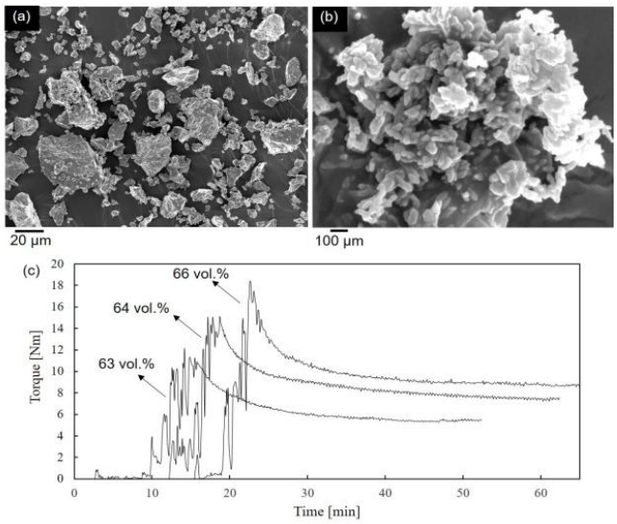

FIGURE 2. (a) Ti6Al4V powder, (b) HA powder and (c) Mixing torque for Ti6Al4V-HA at 63, 64 and 66 vol.% powder loading

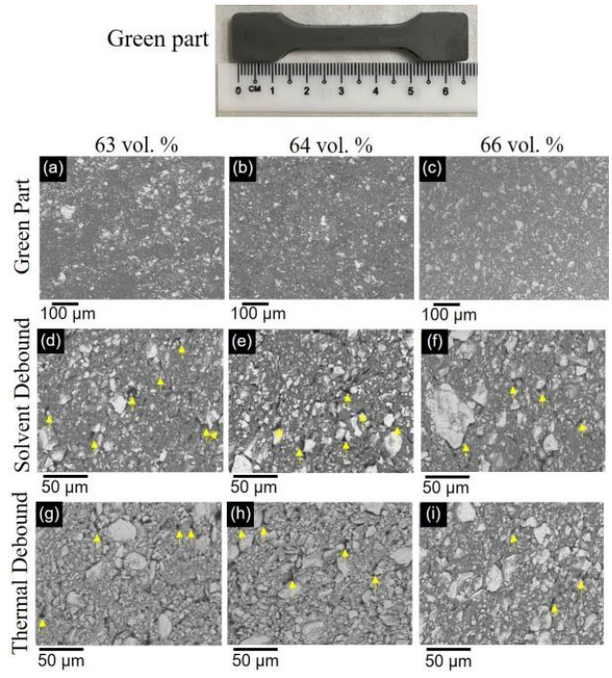

FIGURE 3. SEM image of green part at (a) 63 vol.%, (b) 64 vol.% and (c) 66 vol.%, solvent debound part at (d) 63 vol.%, (e) 64 vol.% and (f) 66 vol.%, and thermal debound part at (g) 63 vol.%, (h) 64 vol.% and (i) 66 vol.%

enhance healing process through cell ingrowth. Porous Ti6Al4V by using space holder technique had average pore size 485 to 572 μm had Young's modulus range from 1.42 to 14.7 GPa (Esen & Bor 2011). Meanwhile, in other literature, porous CP Ti was fabricated by spark plasma sintering (SPS) with pore size of 125 to 800 μm had Young's modulus at 6.2 to 36.1 GPa (Zhang, Otterstein & Burkel 2010). Chen et al. (2009) fabricated porous Titanium by using sodium chloride as space holder via PIM route had pore size up to 300 μm and Young's modulus range from 0.28 to 3.03 GPa. Based on previous study reported on Ti-based porous structure had Young's modulus range from 1.42 to 36.1 GPa, whereas current study obtained 11 GPa which was within the reported range. A porous structure is more advantageous for implantation in order to promote high bone density. It has been reported that bone formation is promoted in porous structures as opposed to rough surfaces (Brentel et al. 2006). The porous structure of Ti6Al4V-HA composite fabricated via PIM is promising to be used for biomedical implantation. However, biomechanical properties should be considered due to large porosity will deteriorate the mechanical properties. Higher porosity will increase cell profileration but their biomechanical properties will be decreased (Lu et al. 1999; Xu et al. 2019).

Subsequently, Figure 4(b) depicts XRD pattern of sintered part. The results indicated that no existence of other HA phases after sintering. α-TCP, β-TCP and TTCP phases were not detected in the sintered part. Hence, it could be concluded that smaller particles which were homogenizedly dispersed were HA particles. Meanwhile in other report, HA is partially transformed into α-TCP, β-TCP, and TTCP when sintered at 1300 °C to 1400 °C, while the major phase of HA will still be maintained even when it is sintered up to 1200 °C (Hung et al. 2012). Since there was no other phosphate element was detected in XRD, it can be concluded that current sintering parameter demonstrated the ability to enhance the stability of HA phases even sinter at high temperature which will reduce the rate of decomposition. Studied had been done on the effect of pre-heat treated HA at 700 °C to 1000 °C prior sintering of 1050 °C to 1350 °C on the phase stability of HA. Pre-heated HA demonstrated higher crystallinity which enhance HA to stabilize even at higher temperature (Chin et al. 2015). In addition, the sintering of HA is favourable in air or moisture environment where it increases the stability of HA crystalline during sintering due to the presence of humidity. The dehydroxylation might occur partially where the main phase of HA was maintained when sintering in air or in moisture atmosphere. This means that the presence of hydrogen or oxygen in the air or moisture atmosphere prevents or restricts dehydroxylation while also preventing or restricting HA decomposition. Meanwhile in this work, as there was approximately 3.4 wt.% of binders left in the debound part, illustrated that the presence of hydrogen or oxygen within the left binders enhance the stability of HA during sintering process which restrain the decomposition of HA. It was reported that pre-sintering step significantly restrained the decomposition of HA (Nurul Nadiah et al. 2021a). The decomposition of HA into TCP was unfavourable due to its bio-resorbable property, which would impair HA's main function. Bio-resorbable materials such as tricalcium phosphate, calcium oxide, and calcium carbonate dissolve in the human body and are replaced by advancing tissue when implanted (Dutta Majumdar, Roy Chowdhury & Ghosh 2018). The main phase of HA will aid in the osseointegration properties of the implants and surrounding tissue, lowering the risk of implant failure. Therefore, the homogenized coating of HA particles on the Ti6Al4V further enhanced the tissue-implants bonding. Following that, the new peaks adjacent to the Ti6Al4V peaks were clearly observed. Those adjacent peaks are matched with Ti3Al (α2 phases) detected by JCPDS 01-074-4579. It can be concluded that the precipitation of α2 phases occurred at sintering temperature of 1300 ºC. The formation of Ti3Al as well as TiAl have a potential for industrial applications possess which consisted with three phases of Ti6Al4V, Ti3Al, and TiAl.

The bending strength of sintered Ti6Al4V-HA was determined at 81.6 ± 6.4 MPa. The obtained bending strength in the current study was within the theoretical value of HA (bending strength ranges from 38 - 250 MPa) (Orlovskii, Komlev & Barinov 2002). On the other hand, the Young's modulus obtain was 11.6 ± 1.5 GPa, which is lower than the theoretical value of Ti6Al4V (115 GPa) and HA (35 - 120 GPa). This is because of the porous structure of sintered part. However, it is good to mention that Young's modulus for sintered part was close to the Young's modulus for human bone which is 10 - 30 GPa (Amir et al. 2014; Dutta Majumdar, Roy Chowdhury & Ghosh 2018). Young's modulus of implants is required to as close as possible with the Young's modulus of the bone to reduce the formation of stress shielding phenomenon.

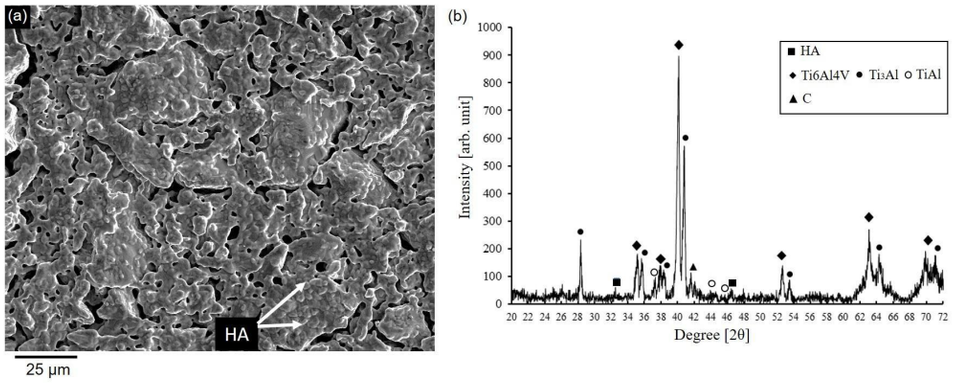

FIGURE 4. (a) SEM image of sintered Ti6Al4V-HA at 1300 °C and (b) XRD pattern for sintered part

CONCLUSION

Several powder loading were developed based on CPVP value of 68 vol.%. Based on the SEM observation of the green parts, the higher the powder loading, the powder and binder distribution became more homogenized. The homogenized feedstock was obtained at powder loading of 66 vol.%. The homogenized distribution of powder and binder could be attributed by the adequate binder and powder ratio in the composition. Subsequently, all the green parts were subjected into solvent and debinding process. The small pores observed in the debound parts of 66 vol.% can be attributed to the homogenized distribution of powder and binder. The smaller pores in the debound part is beneficial to enhance the sinterability of the debound part. Sintered 66 vol.% powder loading exhibited Young's modulus of 11.6 ± 1.5 GPa was within the bone's range (10 to 30 GPa). Young's modulus of the implants is required to as close as the bone's Young's modulus to prevent stress shielding post implantation. The current study demonstrated that Ti6Al4V-HA fabricated using the PIM method has the potential to be used as implant material due to its ability to be injection moulded, had Young modulus within the bone's range, and the main phase of HA was preserved, implying the good osseointegration properties.

ACKNOWLEDGEMENTS

This work was carried out with the assistance from the Ministry of Higher Education, Malaysia (MOHE) under Fundamental Research Grant Scheme (FRGS/1/2021/TK0/UKM/01/2).

REFERENCES

Abdoos, H., Khorsand, H. & Yousefi, A.A. 2014. Torque rheometry and rheological analysis of powder–Polymer mixture for aluminum powder injection molding. *Iranian Polymer Journal (English Edition)* 23(10): 745-755. https://doi.org/10.1007/s13726-014-0268-1

Amir Arifin, Abu Bakar Sulong, Norhamidi Muhamad, Junaidi Syarif & Mohd Ikram Ramli. 2014. Material processing of hydroxyapatite and titanium alloy (HA/Ti) composite as implant materials using powder metallurgy: A review. *Materials and Design* 55: 165-175. https://doi.org/10.1016/j.matdes.2013.09.045

Brentel, A.S., de Vasconcellos, L.M.R., de Vasconcellos, L.G.O., Oliveira, M.V., Cairo, C.A.A., de Alencastro Graca, M.L. & Carvalho, Y.R. 2006. Histomorphometric analysis of pure titanium implants with porous surface versus rough surface. *Journal of Applied Oral Science* 14(3): 213-218.

Chen, L-J., Li, T., Li, Y-M., He, H. & Hu, Y-H. 2009. Porous titanium implants fabricated by metal injection molding. *Transactions of Nonferrous Metals Society of China* 19(5): 1174-1179.

Chin, K.L.J., Chuan, Y.L., Ramesh, S. & Sivakumar, S. 2015. The sinterability of hydroxyapatite bioceramics after undergoing pre-heat treatment. *Journal of Engineering Science and Technology* (Special Issue on SOMCHE 2014 & RSCE 2014 Conference. pp. 83-90.

Crosby, K., Shaw, L.L., Estournes, C., Chevallier, G., Fliflet, A.W. & Imam, M.A. 2014. Enhancement in Ti-6Al-4V sintering via nanostructured powder and spark plasma sintering. *Powder Metallurgy* 57(2): 147-154. https://doi.org/10.1179/1743290113Y.0000000082

Dutta Majumdar, D., Chowdhury, A.R. & Ghosh, M. 2018. Titanium and its alloys for bio-implant applications. *IIM Metal News* 21: 6-9. https://doi.org/10.1002/3527602119.ch16

Eliaz, N. 2019. Corrosion of metallic biomaterials: A review. *Materials* 12(3): 407. https://doi.org/10.3390/ma12030407

Esen, Z. & Bor, S. 2011. Characterization of Ti – 6Al – 4V alloy foams synthesized by space holder technique. *Materials Science and Engineering A* 528: 3200-3209. https://doi.org/10.1016/j.msea.2011.01.008

Faezeh Dalili, Rouhollah Mehdinavaz Aghdam, Reza Soltani & Mohsen Saremi. 2022. Corrosion, mechanical and bioactivity properties of HA-CNT nanocomposite coating on anodized Ti6Al4V alloy. *Journal of Materials Science: Materials in Medicine* 33: Article No. 34. https://doi.org/10.1007/s10856-022-06655-6

Farhana Mohd Foudzi, Norhamidi Muhamad, Abu Bakar Sulong & Hafizawati Zakaria. 2013. Yttria stabilized zirconia formed by micro ceramic injection molding: Rheological properties and debinding effects on the sintered part. *Ceramics International* 39(3): 2665-2674. https://doi.org/10.1016/j.ceramint.2012.09.033

German, R..M. & Bose, A. 1997. *Injection Molding of Metals and Ceramics*. Princeton, New Jersey: Metal Powder Industries Federation.

Hausnerova, B., Kitano, T., Kuritka, I., Prindis, J. & Marcanikova, L. 2011. The role of powder particle size distribution in the processability of powder injection molding compounds. *International Journal of Polymer Analysis and Characterization* 16(2): 141-151. https://doi.org/10.1080/1023666X.2011.547047

Hung, I.M., Shih, W.J., Hon, M.H. & Wang, M.C. 2012. The properties of sintered calcium phosphate with [Ca]/[P] = 1.50. *International Journal of Molecular Sciences* 13: 13569-13586. https://doi.org/10.3390/ijms131013569

Kohri, M., Cooper, E.P., Ferracane, J.L. & Waite, D.F. 1990. Comparative study of hydroxyapatite and titanium dental implants in dogs. *Journal Oral Maxillofacial and Surgery* 48: 1265-1273.

Krishna, E.S. & Suresh, G. 2022. Bioactive titanium-hydroxyapatite composites by powder metallurgy route. *Biointerface Research in Applied Chemistry* 12(4): 5375-5383.

Lin, D., Park, J.M., Kang, T.G., Chung, S.T., Kwon, Y.S. & Park, S.J. 2018. Powder injection molding of Ti-6Al-4V alloy for defect-free high performance titanium parts with low carbon/oxygen contents. *Key Engineering Materials* 770: 189-194. https://doi.org/10.4028/www.scientific.net/KEM.770.189

Lu, J.X., Flautre, B., Anselme, K., Hardouin, P., Gallur, A., Descamps, M. & Thierry, B. 1999. Role of interconnections in porous bioceramics on bone recolonization *in vitro* and *in vivo*. *Journal of Materials Science: Materials in Medicine* 10: 111-120.

McGregor, D.B., Baan, R.A., Partensky, C., Rice, J.M. & Wilbourn, J.D. 2000. Evaluation of the carcinogenic risks to humans associated with surgical implants and other foreign bodies - A report of an IARC monographs programme meeting. *European Journal of Cancer* 36: 307-313. https://doi.org/10.1016/S0959-8049(99)00312-3

Meshalkin, V.P. & Belyakov, A.V. 2020. Methods used for the compaction and molding of ceramic matrix composites reinforced with carbon nanotubes. *Processes* 8: 1-37. https://doi.org/10.3390/PR8081004

Miranda, G., Araújo, A., Bartolomeu, F., Buciumeanu, M., Carvalho, O., Souza, J.C.M., Silva, F.S. & Henriques, B. 2016. Design of Ti6Al4V-HA composites produced by hot pressing for biomedical applications. *Materials and Design* 108: 488-493. https://doi.org/10.1016/j.matdes.2016.07.023

Mohd Yusuf Zakaria, Mohd Ikram Ramli, Abu Bakar Sulong, Norhamidi Muhamad & Muhammad Hussain Ismail. 2021. Application of sodium chloride as space holder for powder injection molding of alloy titanium–hydroxyapatite composites. *Journal of Materials Research and Technology* 12: 478-486. https://doi.org/10.1016/j.jmrt.2021.02.087

Najlaa Nazihah Mas'ood, Farhana Mohd Foudzi, Abu Bakar Sulong, Norhamidi Muhamad & Intan Fadhlina Mohamed. 2018. Two component materials in powder metallurgy: A review paper focused on the processing technique applied in powder metallurgy. *Jurnal Kejuruteraan S1* 1(6): 23-31.

Niespodziana, K. 2019. Synthesis and properties of porous Ti-20 Wt.% HA nanocomposites. *Journal of Materials Engineering and Performance* 28(2): 1-11. https://doi.org/10.1007/s11665-019-03966-8

Niinomi, M. 2002. Recent metallic materials for biomedical applications. *Metallurgical and Materials Transactions A* 33(3): 477-486.

Nurul Nadiah Mahmud, Sulong, A.B., Sharma, B. & Ameyama, K. 2021a. Presintered titanium-hydroxyapatite composite fabricated via pim route. *Metals* 11(2): 318. https://doi.org/10.3390/met11020318

Nurul Nadiah Mahmud, Farah 'Atiqah Abdul Azam, Mohd Ikram Ramli, Farhana Mohd Foudzi, Kei Ameyama & Abu Bakar Sulong. 2021b. Rheological properties of irregular-shaped titanium-hydroxyapatite bimodal powder composite moulded by powder injection moulding. *Journal of Materials Research and Technology* 11: 2255-2264. https://doi.org/10.1016/j.jmrt.2021.02.016

Okazaki, Y. & Gotoh, E. 2005. Comparison of metal release from various metallic biomaterials *in vitro*. *Biomaterials* 26(1): 11-21. https://doi.org/10.1016/j.biomaterials.2004.02.005

Orlovskii, V.P., Komlev, V.S. & Barinov, S.M. 2002. Hydroxyapatite and hydroxyapatite-based ceramics. *Inorganic Materials* 38(10): 973-984. https://doi.org/10.1023/A:1020585800572

Otsuki, B., Takemoto, M., Fujibayashi, S., Neo, M., Kokubo, T. & Nakamura, T. 2006. Pore throat size and connectivity determine bone and tissue ingrowth into porous implants: Three-dimensional micro-CT based structural analyses of porous bioactive titanium implants. *Biomaterials* 27: 5892-5900. https://doi.org/10.1016/j.biomaterials.2006.08.013

Supati, R., Loh, N.H., Khor, K.A. & Tor, S.B. 2000. Mixing and characterization of feedstock for powder injection molding. *Materials Letters* 46(2-3): 109-114. https://doi.org/10.1016/S0167-577X(00)00151-8

Tecu, C., Antoniac, A., Goller, G., Gok, M.G., Manole, M., Mohan, A., Moldovan, H. & Earar, K. 2018. The sintering behaviour and mechanical properties of hydroxyapatite - Based composites for bone tissue regeneration. *Revista de Chimie* 69(5): 1272-1275. https://doi.org/10.37358/rc.18.5.6306

Thavanayagam, G., Pickering, K.L., Swan, J.E. & Cao, P. 2015. Analysis of rheological behaviour of titanium feedstocks formulated with a water-soluble binder system for powder injection moulding. *Powder Technology* 269: 227-232. https://doi.org/10.1016/j.powtec.2014.09.020

Thomas-vielma, P., Cervera, A., Levenfeld, B. & Varez, A. 2008. Production of alumina parts by powder injection molding with a binder system based on high density polyethylene. *Journal of European Ceramic Society* 28: 763-771. https://doi.org/10.1016/j.jeurceramsoc.2007.08.004

Xu, W., Lu, X., Muhammad Dilawer Hayat, Tian, J., Huang, C., Chen, M., Qu, X. & Wen, C. 2019. Fabrication and properties of newly developed Ti35Zr28Nb scaffolds fabricated by powder metallurgy for bone-tissue engineering. *Journal of Materials Research and Technology* 8(5): 3696-3704. https://doi.org/10.1016/j.jmrt.2019.06.021

Zhang, B.F., Otterstein, E. & Burkel, E. 2010. Spark plasma sintering, microstructures, and mechanical properties of macroporous titanium foams. *Advanced Engineering Materials* 9: 863-872. https://doi.org/10.1002/adem.201000106.

*Corresponding author; email: nn90.kawai@gmail.com